Aspects of Large Area CIGS Technology

A. Delahoy, M. Akhtar, J. Cambridge, L. Chen, D. Chorobski, R. Govindarajan,
S. Guo, Z. Kiss, A. Ruppert, J.A. Anna Selvan, F. Ziobro

Energy Photovoltaics, Inc.
Princeton, NJ 08543

ABSTRACT

This paper singles out results from several programs aimed at carrying CIGS technology into new arenas. These programs include large area vacuum deposition, high V_{oc} devices, ZIS buffer layers, and a-Si/CIGS tandem modules.

1. Introduction

As part of the Thin Film Partnership Program, EPV has conducted research to support a technology base for production of CIGS PV modules based on vacuum deposition onto glass. To prepare CIGS on large glass substrates (currently 0.43m^2, with scale up to 0.79m^2 in progress), EPV delivers materials (including Cu) from line sources to a substrate that is translated in a direction perpendicular to the axis of the source. This brief paper describes certain aspects of this work, including flux distribution from linear sources, layer and device uniformity, high V_{oc} devices, and evaporation of $ZnIn_2Se_4$ for buffer layers. Preliminary internal results concerning the fabrication of advanced a-Si/CIGS tandem devices are also presented.

2. Large area deposition

We had earlier conducted modeling of our linear sources assuming an infinite line source of constant strength and a cosine law emission from each element of the source. Experimentally, a more peaked thickness distribution was found [1]. We have now repeated the calculation for a $\cos^3(\theta)$ emission law, and find that for a source-to-substrate distance h, and a mass emission rate m_e, the film mass m(p) at a distance p along the substrate is

$$m(p) = \tfrac{3}{4}\, m_e\, h^4/(h^2 + p^2)^{5/2} \qquad (1)$$

Even better agreement with experiment is found for a $\cos^{3.5}(\theta)$ emission law. This is shown in Figure 1, which shows the normalized thickness for a Se film deposited onto a stationary substrate from a linear source (solid data points) and the result of the flux integration (curve).

For CIGS films prepared by translating the substrate under the sources, Figure 2 shows the composition ratios Cu/(In+Ga) and Ga/(In+Ga), as determined in-house by ICP, as a function of distance along the substrate i.e. in a direction normal to the source axes. Good uniformity is obtained. The figure also maps diagnostic device parameters V_{oc}, FF and efficiency along the plate. It would appear that FF is controlled by a factor that is not directly related to composition.

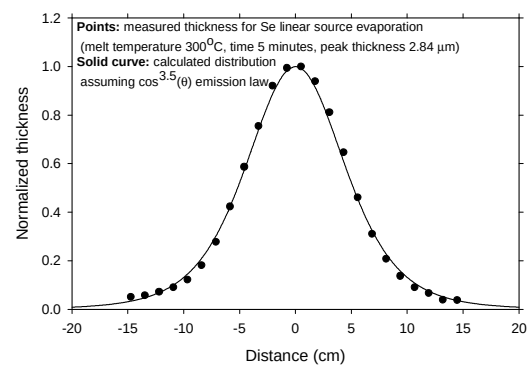

Fig. 1. Experimental and modeled thickness profiles for linear source evaporation.

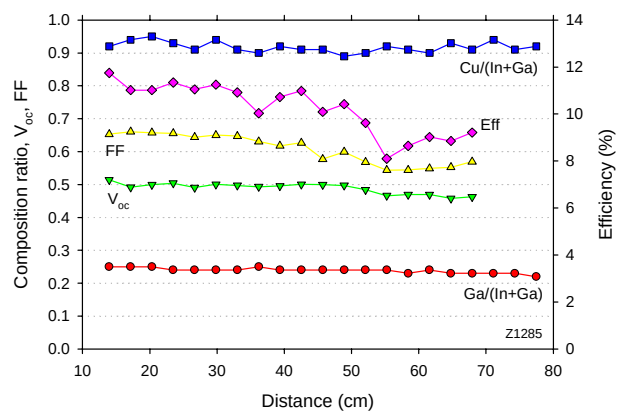

Fig. 2. CIGS composition and device parameters as a function of position along the plate.

3. High V_{oc} devices

High Ga content material has also been produced over large areas by linear source evaporation. Figure 3 (overleaf) shows the I-V curve of an 11.2% diagnostic device with 596 mV V_{oc} and 67.7% fill factor prepared in run Z1301. The composition of the CIGS is shown in Table 1 below. High voltage, lower current devices such as these are particularly suitable for modules.

Table 1. Film composition obtained by ICP

Sample	Cu (%)	In (%)	Ga (%)	Se (%)	Cu/(In +Ga)	Ga/(In +Ga)
Z1301	21.4	14.7	12.0	51.9	0.80	0.45
H89	15.5	22.1	8.9	53.6	0.50	0.29
H93	22.9	17.9	8.5	50.7	0.87	0.32

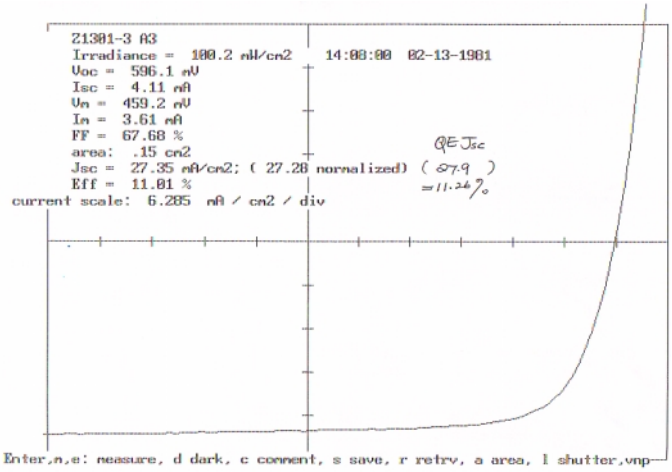

Fig. 3. I-V curve for 11.2% cell prepared using pilot line CIGS with Ga/(In+Ga) = 0.45.

4. Use of $ZnIn_2Se_4$

We have previously reported the synthesis and use of $ZnIn_2Se_4$ as a source material for ZIS buffer layer deposition [2]. Here we report the deposition rate of ZIS as a function of source temperature during the complete evaporation of a fresh charge of $ZnIn_2Se_4$. A small emission peak was discovered at a source temperature of about 290°C, followed by the principal emission peak at about 850-860°C, with no other peaks at higher temperatures (see Figure 4). Analysis of material (in-house by EDS) captured on a glass slide during the initial emission revealed it to be selenium.

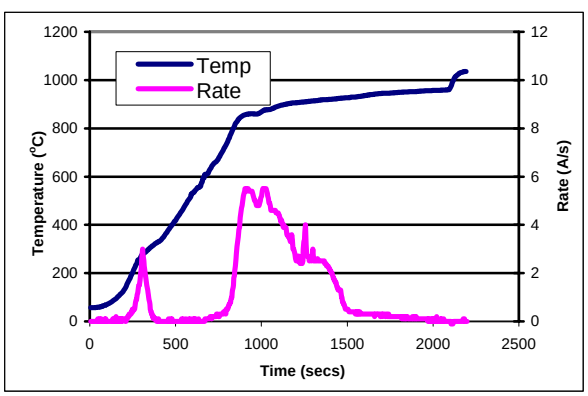

Fig. 4. ZIS deposition rate as a function of evaporation time and source temperature.

The quantum efficiency of device ZIS26-A2 with a ZIS buffer layer is compared in Fig. 5 to the QE of two R&D devices using standard CBD CdS. (The long-wavelength QE of the CdS devices is controlled, not by global Ga content, but by Ga content in the junction region.)

5. a-Si/CIGS tandem devices

As a manufacturer of same-bandgap, a-Si/a-Si thin film modules (the EPV-40, 40W, 0.79m^2) and Integrated Manufacturing Systems, EPV is interested in the lamination of monolithic a-Si plates to CIGS plates to form a-Si/CIGS tandem modules. We calculate that, in this way, a 8% CIGS module can be turned into a 10.4% a-Si/CIGS module.

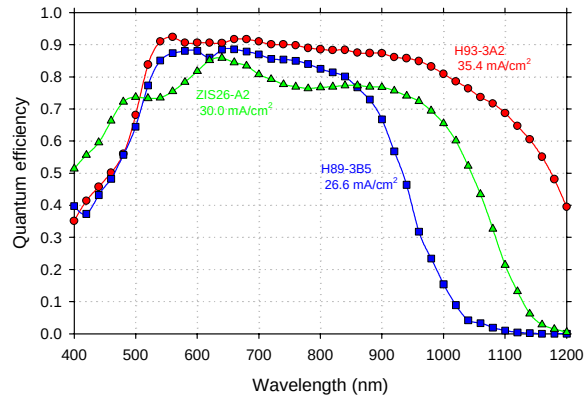

Fig. 5. Quantum efficiency of CIGS devices with ZIS and CdS buffer layers and different band gaps.

Previous attempts to develop this technology were stymied by large parasitic absorption of light intended for the CIGS plate. We have started a program to understand and solve this problem. If a filter consisting of soda-lime glass/SnO_2:F/a-Si/ZnO:Al is simply placed in front of a bare CIGS device with J_{sc} of 34.8 mA/cm^2, the J_{sc} of the CIGS device is massively reduced to 5.6 mA/cm^2. By various means, we have reduced the losses so that a J_{sc} of 12.9 mA/cm^2 is obtained (Fig. 6).

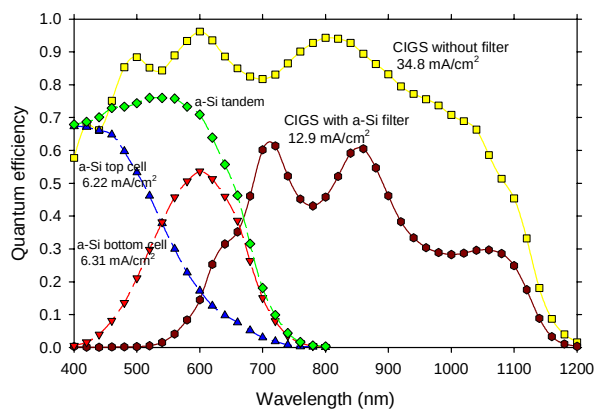

Fig. 6. Quantum efficiency of filtered and un-filtered CIGS devices, with QE of tandem a-Si for comparison.

ACKNOWLEDGMENTS

The authors thank the other members of EPV's technical staff who contributed to this work, and the US DOE for support under subcontract ZAK-8-17619-21 with NREL.

REFERENCES

[1] A. Delahoy, J. Bruns, L. Chen, M. Akhtar, Z. Kiss. "Advances in Large Area CIGS Technology," *Proc. 28th IEEE PV Specialists Conference*, September 15-22, 2000, Anchorage, AK, pp. 1437-1440.

[2] A. Delahoy, M. Akhtar, J. Bruns, A. Ruppert, L. Chen, Z. Kiss. "Ternary Source Materials for CIGS Buffer Layers," *Proc. 16th European PVSEC*, 1-5 May 2000, Glasgow, UK, pp. 767-770.